Characterization of Focal EEG Signals: A Review

U Rajendra Acharya[1,2,3,*], Yuki Hagiwara[1], Sunny Nitin Deshpande[1], S Suren[1], Joel En Wei Koh[1], Shu Lih Oh[1], N Arunkumar[4], Edward J Ciaccio[5], Choo Min Lim[1]

[1] Department of Electronics and Computer Engineering, Ngee Ann Polytechnic, Singapore.

[2] Department of Biomedical Engineering, School of Science and Technology, Singapore University of Social Sciences, Singapore.

[3] School of Medicine, Faculty of Health and Medical Sciences, Taylor's University, Subang Jaya, Malaysia.

[4] Department of Electronics and Instrumentation, SASTRA University, Thanjavur, India.

[5] Department of Medicine, Columbia University, New York, USA.

*Corresponding Author:

Postal Address: Department of Electronics and Computer Engineering, Ngee Ann Polytechnic, Singapore 599489.

Telephone: +65 6460 6135; Email Address: aru@np.edu.sg

ABSTRACT

Epilepsy is a common neurological condition that can occur in anyone at any age. Electroencephalogram (EEG) signals of non-focal (NF) and focal (F) types contain brain activity information that can be used to identify areas affected by seizures. Generally, F EEG signals are recorded from the epileptic part of the brain, while NF EEG signals are recorded from brain regions unaffected by epilepsy. It is essential to correctly detect F EEG signals, when and where they occur, as focal epilepsy can be successfully treated by surgical means. However, all EEG signals are complex and require highly trained personnel for right interpretation. To overcome the associated challenges, in this study a computer-aided detection (CAD) system to aid in the detection of F EEG signals has been developed, and the performance of nonlinear features for differentiating F and NF EEG signals is compared. Moreover, it is noted that nonlinear features can effectively capture concealed patterns and rhythms contained in the EEG signals. Overall, it was found that the CAD system will be useful to clinicians in providing an accurate and objective paradigm for localization of the epileptogenic area.

Keywords – Computer-aided detection system; electroencephalogram signals; epilepsy; focal; non-focal.

1. Introduction

Epilepsy is a persistent brain disorder that can afflict anyone at any age [1]. It is defined as the occurrence in a patient of two or more unprovoked seizures. Seizures occur due to the excessive electrical discharges of brain cells. As stated by the World Health Organization, currently, nearly 50 million people globally suffer from epilepsy [2]. This condition affects the patient socially as well as economically [2]. It has been reported that epilepsy attributes to approximately 0.6% of the global burden of disease. Nonetheless, patients suffering from epilepsy can lead a normal life with the appropriate treatment. Therefore, it is crucial to be able to correctly diagnose epilepsy and to administer the right treatment to the patient.

The electroencephalogram (EEG) records brain activity from the scalp and can be used to diagnose epilepsy. Quantitative analysis of EEG characteristics can be helpful to diagnose the condition. Magnetic resonance imaging (MRI) is another modality useful in the diagnosis of epilepsy. Currently, EEG is the preferred data type employed for epilepsy diagnosis due to its low cost.

Focal epilepsy is a form of the condition that occurs in certain brain areas [3]. The focal (F) EEG signals are acquired from this region, where the first ictal EEG changes are observed. Non-focal (NF) EEG signals are obtained from brain regions that do not contribute to seizure onset. Both F and NF EEG signals lack seizure segments [3]. It is reported that greater than 20% of patients are affected by generalized epilepsy which manifest from the entire brain, while more than 60% of patients suffer from focal (partial) epilepsy, localized to a smaller region of the brain [3]. It is difficult to treat patients with focal epilepsy by medication alone [3]; hence the need to localize the epileptic zone. Thus, detection and discernment of F and NF signals is an important area of quantitative research in this field, as the localization of epileptogenic regions is crucial for successful epilepsy surgery. Since treatment of focal epilepsy often involves removal of the affected brain area surgically [4], it is crucial to discern F EEG signals and their origin.

Substantial research work has been done thus far to characterize F versus NF signals. Typically, F EEG signal morphology is characterized by more rhythmic and less chaotic behavior as compared to NF EEG signals [5]. However, it is challenging to identify the EEG signals visually, due to the presence of low amplitude and random components. Thus, computer-aided detection (CAD) systems have been proposed to develop an automated tool for aid in the identification of EEG characteristics. Several have thus far been conducted, summarized in Table 2. Sharma et al.

[6] decomposed EEG signals with an empirical mode decomposition (EMD) technique and extracted entropy features. Their group found an accuracy for EEG classification of 87%. In their subsequent work, they analyzed the signals using the discrete wavelet transform (DWT), and extracted entropy features from the decomposed signals [7]. This approach yielded an accuracy of 84 ± 11%. In their latest study, they utilized the tunable-Q wavelet transform (TQWT) prior to extraction of entropy features. This novel decomposition technique achieved a diagnostic accuracy of 95% [8].

Deivasigamani et al. [9] proposed a dual-tree complex wavelet transform (DTCWT) method to decompose EEG signals and obtained mean and standard deviation (SD) values from the decomposed coefficients. They reported a sensitivity of 98% and specificity of 100% in classifying the signals into F and NF classes. Das et al. [10] combined two decomposition methods, namely the EMD and DWT, and applied these methods to the data. Entropy features were once again extracted and were then classified with an accuracy of 89%. Sharma et al. [11] employed a wavelet filter bank and an entropy feature extraction algorithm to separate NF from F EEG signals. The method accuracy was 94%.

Gupta et al. [12] applied the flexible analytic wavelet transform (FAWT) and subjected the signals to a maximum of 15 levels of decomposition. They then extracted entropy features from the coefficients and characterized them into two classes. They obtained a sensitivity and specificity of 93% and 96%, respectively. Bhattacharrya et al. [13] employed TQWT for decomposition and extracted entropy features from the EEG data to achieve an accuracy of 85%. In their subsequent study, Bhattacharrya et al. [14] proposed to decompose the EEG signals into rhythms using the empirical wavelet transform (EWT), and subjected these rhythms to a reconstructed phase space (RPS) analysis to distinguish between F and NF signals. Their novel algorithm yielded a sensitivity and specificity of 88% and 92%, respectively. Sriraam et al. [15] investigated the capabilities of multi-features in the differentiation of NF and F signals. They adopted statistical, frequency-based, and nonlinear feature extractors. It was reported that the integration of different features could localize the epileptogenic areas of the brain with an accuracy of 92%. Arunkumar et al. [16] extracted several entropy features, and subjected these features to a non-nested generalized exemplars classifier. Their methodology achieved an accuracy level of 98%.

It can be noted from Table 2 that nonlinear features are commonly employed for epilepsy analysis. The motivation of our study is to evaluate the performances of the nonlinear features utilized in the CAD algorithm. The entire database is employed to extract widely used nonlinear features.

These nonlinear features have shown clear separation between the two groups. Also, unique recurrence, bispectrum and cumulant plots are used for class separation. Moreover, the challenges associated with the CAD system, and future developments, are discussed.

2. Data Types Used for Analysis

The EEG signals discussed herein were obtained from the publicly available Bern-Barcelona EEG database [5]. They were collected at the Department of Neurology of the University of Bern from five patients suffering from epilepsy. The patients underwent long-term intracranial EEG recording with intracranial strip and depth electrodes. All patients had been diagnosed with longstanding pharmacoresistant temporal lobe epilepsy.

A total of 3,750 F EEG signals and 3,750 NF EEG signals were used in this study (N = 10,240 samples per signal). The database consists of bivariate EEG signals in the X and Y time series. Figure 1 shows an example of F and NF EEG signals in the X-series, Y-series and X-Y series respectively.

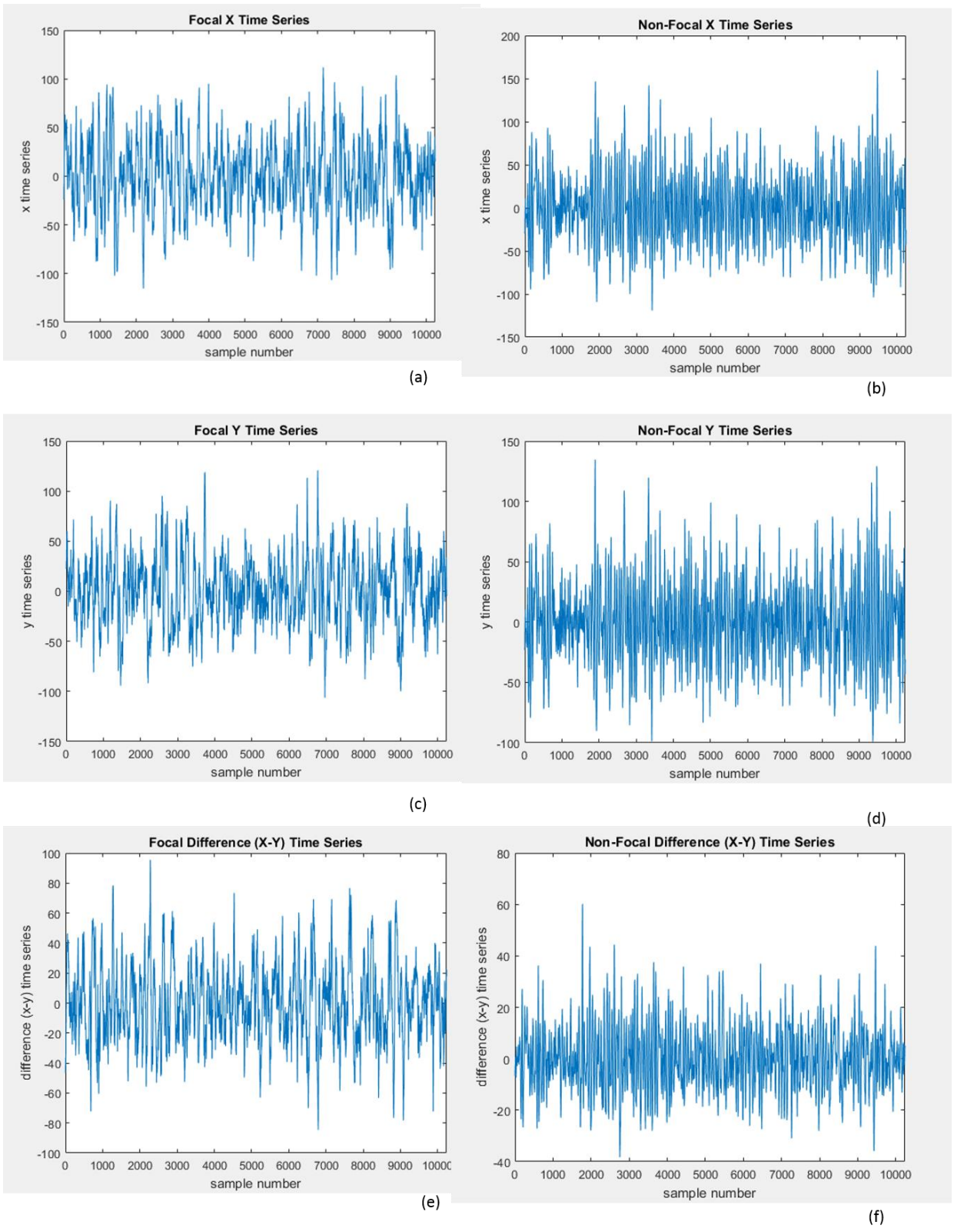

Figure 1: A sample of (a) F and (b) NF EEG signal in the X-series, (c) F and (d) NF EEG signals in the Y-series, and (e) F and (f) NF EEG signals in the X-Y series.

3. Computer-Aided Detection System

The CAD system is employed to investigate the effectiveness of the various feature extraction techniques in the detection of NF and F EEG signals. Figure 2 is a typical block diagram of the development of a CAD system. It encompasses the input of NF and F EEG signals followed by the pre-processing of the signals. Thereafter, several feature extraction methods are implemented to obtain useful and discriminative characteristics. These features are ranked according to their statistical significance. Lastly, the highest-ranked features are input to the classifier.

The subsequent sections describe the different processes within the CAD systems.

Figure 2: A typical block diagram of a CAD system.

3.1 Pre-processing

Usually, EEG signals are subjected to pre-processing for removal of artifacts and noise prior to feature extraction. However, no pre-processing was performed in this study, as the signals are already pre-processed when downloaded from the database. Nonetheless, we have subjected these signals to a differencing operation to obtain the EEG signals in the X-Y series (see Figure 1(e) and (f)) before the extraction of features [17].

3.2 Extraction of Nonlinear Features

In this study, *nine* nonlinear features were extracted and compared. The use of nonlinear features can be helpful to describe salient properties of EEG signal morphology, which tend to appear

complex and chaotic [18]. Extraction of such nonlinear features has been widely implemented to determine the important characteristics of EEG signals [18].

a. Detrended Fluctuation Analysis (DFA)

The DFA is often used to detect inherent self-similarity characteristics of the EEG [19]. The variant of the DFA, namely the root mean square (RMS) multi-fractal DFA is implemented together with the DFA feature.

b. Entropies

The entropy feature is useful to evaluate the uncertainty and irregularity present in EEG signals [20]. In general, the entropy of the EEG signal is higher when the variability and complexity of the EEG signals increases.

The entropy types extracted in this study are the modified multi-scale entropy (MMSE) with *ten* scales employed [21], sample [22], approximate [23], fuzzy [24], Kolmogorov-Sinai [25], Renyi [26], Shannon [27], bispectrum entropy 1, bispectrum entropy 2, and bispectrum phase entropy [28], Tsallis [29], wavelet [30], and permutation [31].

c. Fractal Dimension (FD)

The fractal dimension or FD metric [32] can be utilized to compare the complexity of details in the EEG. Hence, it enables detection of EEG signal patterns and details that may not be evident visually.

d. Hjorth

There are three Hjorth parameters, namely the mobility, complexity, and activity, which are used to quantify EEG signal morphology [33].

e. Hurst Exponent

The Hurst exponent [34] is an estimation of predictability and self-similarity in the EEG. A greater magnitude for the Hurst exponent is indicative of a smoother and less complicated EEG signal.

f. Kolmogorov Complexity

This parameter describes the characteristics of the EEG signals [35]. Therefore, the more random the signals are, the longer is the length of the description.

g. Largest Lyapunov Exponent (LLE)

The LLE is computed to obtain an estimate of the degree of chaos present in the signals [36]. Therefore, it is noted that the higher the LLE value, the more complex the signals are.

h. Lempel-Ziv Complexity (LZC)

The LZC [37] is used to measure the repetitiveness of the EEG signals. Hence, the more repetitive the signal, the higher the LZC value.

i. Recurrence Qualitative Analysis (RQA)

The RQA measures the number of times of recurrences in order to evaluate the complexity of the EEG signals [38]. The parameters of the RQA include laminarity, transitivity, determinism, trapping time, the entropy of diagonal line lengths, mean diagonal line length, maximal vertical line length, maximal diagonal line length, recurrence time (1^{st} type and 2^{nd} type), recurrence time entropy, and the recurrence rate [39, 38, 40, 41].

3.3 Feature Ranking

Extracted features can be ranked according to the student t-test, corresponding to the level of statistical significance [42]. In reference to the literature (see Table 2), several other feature ranking techniques, namely the receiver operating characteristic (ROC) approach [43], Bhattacharyya distance [44], Wilcoxon test [45], the Kullback-Leibler distance [43], and the Kruskal-Wallis test [46], may also be used to order extracted features according to level of significance.

3.4 Classification

Classification is the last step in the formation of the CAD system. Based upon the literature (see Table 2), the most commonly used classifier is the least squares-support vector machine (LS-SVM) [47]. However, the adaptive neuro-fuzzy inference system (ANFIS) [48], k-nearest neighbor (KNN) [49], and the non-nested generalized exemplars [50] classifiers are also used. Herein, the LS-SVM classifier using polynomial 3 is implemented in accord with the majority of published work, which uses this classifier. Also, the 10-fold cross-validation strategy is adopted in this study.

4. Results

In this study, nonlinear features were extracted from EEG signals. When 23 features were extracted using the LS-SVM for classification, the maximum accuracy of 87.93% was obtained, with a sensitivity and specificity of 89.97% and 85.89%, respectively. All extracted features are listed in Table 1 in descending order according to statistical significance. It is noted that all 52 F and NF features recorded in the table have a p-value of < 0.01.

According to Table 1, the MMSE is highest ranked. This implies that the MMSE is the most statistically significant as compared to other features. MMSE quantifies the pattern and detects regularity in the EEG signals. It can be noted that most of the entropy features have higher values for NF than for F EEG signals. This is typically caused by the F EEG signals being more periodic and less random. Figure 3 is a graphical representation of the top ten extracted features. Higher mean values are evident for NF as compared to F EEG signals.

The RQA features in Table 1 reflect higher values in the F class as compared to the NF class. This is because the RQA evaluates the number of patterns and occurrences of spikes and subtle changes in the EEG signals, which are more present in F EEG. Thus, the more rhythmic focal EEG signals result in higher mean RQA parameters, which can be useful identify concealed signal patterns. Similarly, the DFA features portray higher values in the F class versus NF class, as the DFA parameter detects rhythmic patterns present in the signals.

Figures 4 to 6 display the typical recurrence, bispectrum, and cumulant plots of F and NF EEG signals, respectively. The F recurrence plot in Figure 4 appears more periodic and homogenous, whereas the NF recurrence plot portrays a more random and inconsistent depiction. In Figure 5, the two plots are unique, displaying different characteristics. The amplitudes of the F bispectrum are larger, while the NF bispectrum plot reflects the presence of smaller amplitudes. Additionally, the F plot has more consistent peaks as compared to the NF plot. This means that the bispectrum features in the F plot are more periodic and regular. Similarly, the F cumulant plot has higher amplitudes than the NF cumulant plot in Figure 6.

These figures indicate that the extracted nonlinear features (recurrence, bispectrum, and cumulants) can be efficaciously utilized for classification, and that they provide visually apparent distinctions between the two classes.

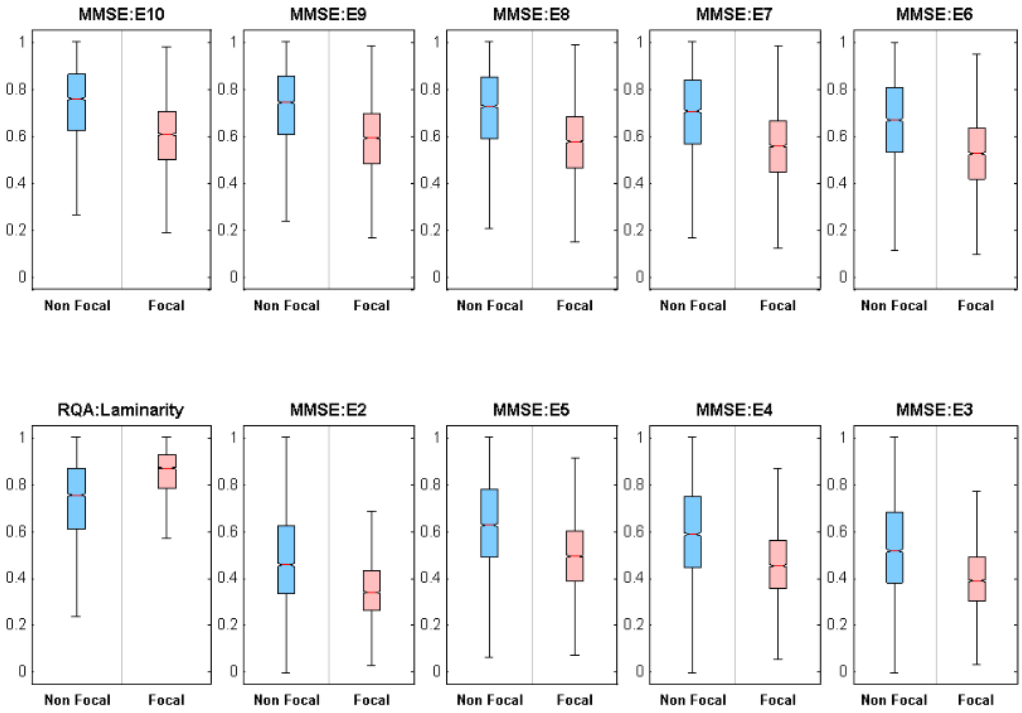

Figure 3: The top 10 highly-ranked features extracted from the two classes of EEG signals, with their corresponding mean and SD values.

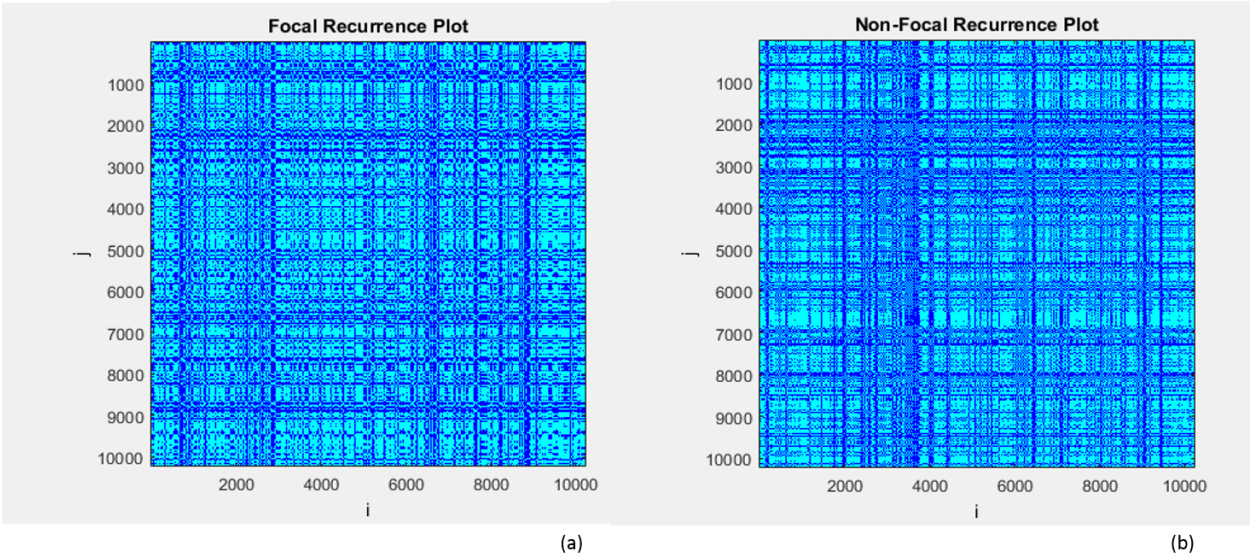

Figure 4: A sample of (a) F and (b) NF X-Y difference recurrence plots.

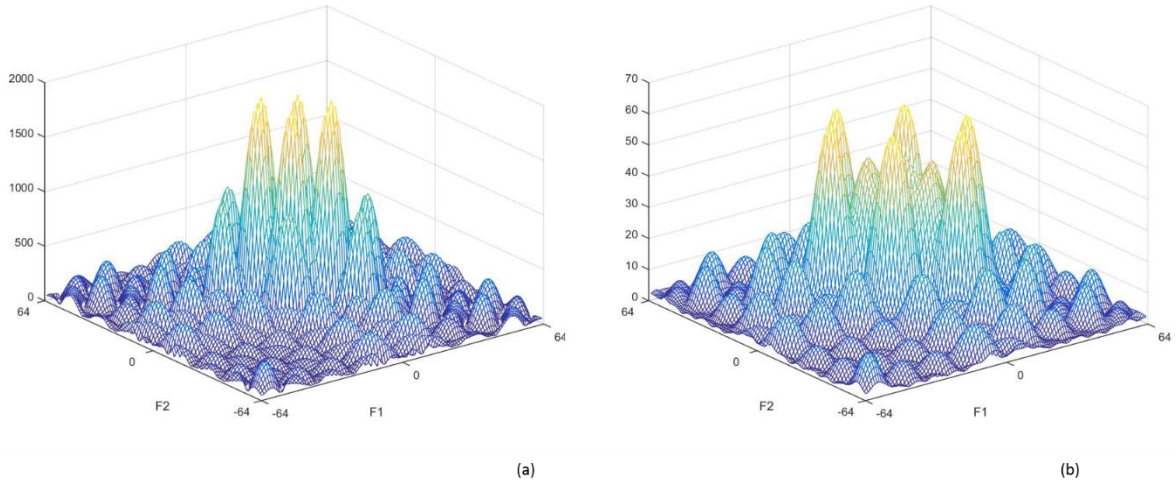

Figure 5: A sample of (a) F and (b) NF X-Y difference bispectrum plots.

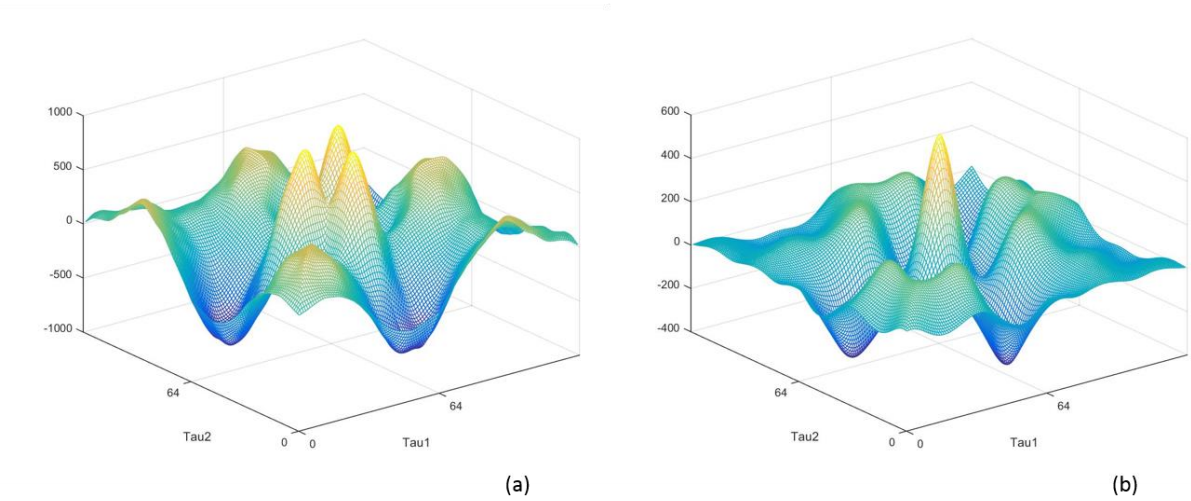

Figure 6: A sample of (a) F and (b) NF X-Y difference cumulants plots.

Table 1: The mean and SD value of the extracted features, $p < 0.01$.

No.	Features extracted	F Mean ± SD	NF Mean ± SD
1	MMSE: E10	0.659 ± 0.128	0.768 ± 0.140
2	MMSE: E9	0.646 ± 0.130	0.757 ± 0.145
3	MMSE: E8	0.633 ± 0.133	0.747 ± 0.150

4	MMSE: E7	0.615 ± 0.135	0.731 ± 0.156
5	MMSE: E6	0.585 ± 0.135	0.700 ± 0.160
6	RQA: Laminarity	0.856 ± 0.0973	0.756 ± 0.155
7	MMSE: E2	0.397 ± 0.124	0.511 ± 0.174
8	MMSE: E5	0.551 ± 0.135	0.665 ± 0.165
9	MMSE: E4	0.512 ± 0.135	0.627 ± 0.173
10	MMSE: E3	0.448 ± 0.129	0.562 ± 0.173
11	MMSE: E1	0.372 ± 0.118	0.476 ± 0.157
12	RQA: Determinism	0.742 ± 0.127	0.634 ± 0.166
13	Sample entropy	0.581 ± 0.0795	0.651 ± 0.111
14	Approximate entropy	0.591 ± 0.120	0.688 ± 0.157
15	RQA: Entropy of diagonal line lengths	0.492 ± 0.0903	0.428 ± 0.100
16	Fuzzy entropy	0.420 ± 0.106	0.508 ± 0.175
17	DFA	0.772 ± 0.0673	0.728 ± 0.0833
18	RQA: Trapping time	0.275 ± 0.0725	0.237 ± 0.0616
19	RQA: Mean diagonal line length	0.324 ± 0.0606	0.293 ± 0.0535
20	RQA: Maximal vertical line length	0.122 ± 0.0781	0.0865 ± 0.0542
21	RQA: Recurrence time 2nd type	0.273 ± 0.0916	0.224 ± 0.0941
22	Kolmogorov-Sinai entropy	0.409 ± 0.238	0.298 ± 0.231
23	RQA: Recurrence time entropy	0.719 ± 0.0579	0.693 ± 0.0564
24	Hjorth mobility	0.210 ± 0.0776	0.247 ± 0.108
25	RQA: Transitivity	0.974 ± 0.00170	0.974 ± 0.00130
26	Renyi entropy	0.783 ± 0.0677	0.761 ± 0.0711
27	Shannon entropy	0.0709 ± 0.0910	0.0483 ± 0.0466
28	RQA: Maximal diagonal line length	0.0260 ± 0.0501	0.0149 ± 0.0388
29	RQA: Recurrence time 1st type	0.869 ± 0.0889	0.884 ± 0.0779
30	Bispectrum: Entropy 2	0.370 ± 0.107	0.393 ± 0.138
31	FD	0.635 ± 0.0450	0.645 ± 0.0599

32	RQA: Recurrence rate	0.332 ± 0.0467	0.325 ± 0.0366
33	Kolmogorov complexity	1 ± 0	1 ± 0.001
34	Bispectrum: Entropy 1	0.581 ± 0.0868	0.595 ± 0.114
35	RMS Multi-Fractal DFA 10	0.0915 ± 0.0869	0.0799 ± 0.0838
36	RMS Multi-Fractal DFA 6	0.0798 ± 0.0730	0.0701 ± 0.0740
37	Tsallis entropy	0.0305 ± 0.0523	0.0243 ± 0.0433
38	RMS Multi-Fractal DFA 5	0.0776 ± 0.0728	0.0681 ± 0.0754
39	Wavelet entropy	0.0245 ± 0.0493	0.0188 ± 0.0396
40	RMS Multi-Fractal DFA 1	0.0629 ± 0.0567	0.0554 ± 0.0634
41	RMS Multi-Fractal DFA 3	0.0761 ± 0.0709	0.0673 ± 0.0732
42	LLE	0.456 ± 0.19	0.479 ± 0.205
43	RMS Multi-Fractal DFA 2	0.0880 ± 0.0828	0.0779 ± 0.0886
44	Permutation entropy	0.815 ± 0.0571	0.822 ± 0.059
45	RMS Multi-Fractal DFA 8	0.0741 ± 0.0711	0.0659 ± 0.0732
46	Hjorth complexity	0.555 ± 0.0970	0.565 ± 0.0993
47	RMS Multi-Fractal DFA 7	0.0739 ± 0.0700	0.0662 ± 0.0709
48	RMS Multi-Fractal DFA 4	0.0800 ± 0.0726	0.0717 ± 0.0815
49	RMS Multi-Fractal DFA 9	0.0831 ± 0.0733	0.0749 ± 0.0832
50	Hurst exponent	0.758 ± 0.0653	0.754 ± 0.0845
51	LZC	0.500 ± 0.091	0.5 ± 0
52	Bispectrum: Phase entropy	0.971 ± 0.528	0.971 ± 0.530

where E*X* refers to the different scales (1 to 10) of the MMSE feature.

where RMS Multi-Fractal DFA *X* refers to the different scales (1 to 10) of the variant DFA feature.

5. Discussion

Published CAD system algorithms for automatic detection of F EEG signals are summarized in Table 2. It is evident from the table that most of the systems employed various decomposition

techniques prior to the extraction of features. These decomposition approaches include the EMD [51], DWT [52], DT-CWT [53], WFB [54], TQWT [55], FAWT [56], and EWT [57]. Hence, it is noted that a combination of decomposition techniques and nonlinear features have successfully and efficiently been used to characterize F and NF EEG signals.

The entropy feature extraction technique is often used in quantitative epilepsy analysis [6, 7, 10, 8, 11, 12, 13, 15, 16]. This may be because entropy features are simple to implement, and they can also well quantify abrupt changes in EEG morphology. Therefore, it is used as a feature by many investigators during the development of CAD systems.

Nonetheless, Deivasigamani et al. [9] proposed to calculate the mean and SD of the coefficients obtained from the decomposed EEG signals and separate them into their corresponding classes (F or NF). Also, Bhattacharyya et al. [14], instead of extracting entropy features, have utilized the reconstructed phase space (RPS) with central tendency measure (CTM) to differentiate the two classes of EEG signals.

Overall, it can be noted that all *nine* nonlinear features extracted are highly discriminative between F and NF classes, even though entropy features performed better in differentiation.

The main highlights of this study are as follows:

i. This is the first study to compare the performances of many nonlinear features for F and NF EEG signal quantitative analysis.
ii. The nonlinear features are able to recognize subtle patterns present in the EEG signals, and are assistive to characterize them according to their respective classes.
iii. We have utilized the entire EEG database in this review.
iv. Unique recurrence, bispectrum and cumulant plots are proposed to discriminate the two classes of EEG signals visually.

The disadvantages of our findings are:

i. Quantitative analysis for epilepsy is computationally intensive. Incorporation of a graphics processing unit would be useful to better handle the level of complexity during analysis of EEG morphology.
ii. More subjects are required to validate the CAD system. Currently, the database consists of the data from five subjects.

Table 2: A summary of published journal articles using the Bern-Barcelona EEG database for automated detection of F and NF EEG signals.

Authors (year)	Number of signals used	Techniques proposed	Types of cross-validation used	Performance of the proposed algorithm in %		
				Accuracy	Sensitivity	Specificity
Sharma et al. (2015a) [6]	F: 50 NF: 50	EMD, entropy, LS-SVM	10-fold	87	90	84
Sharma et al. (2015b) [7]	F: 50 NF: 50	DWT, entropy, t-test, ROC, Bhattacharyya distance, Wilcoxon test, Kullback-Leibler distance, LS-SVM (Index proposed)	10-fold	84 ± 10.74	84 ± 15.77	84 ± 12.66
Deivasigamani et al. (2016) [9]	F: 50 NF: 50	DT-CWT, mean, SD, ANFIS	-	99	98	100
Das et al. (2016) [10]	F: 50 NF: 50	EMD-DWT, entropy, KNN	-	89.40	90.70	88.10
Sharma et al. (2017) [8]	F: 3,750 NF: 3,750	WFB, entropy, t-test, LS-SVM	10-fold	94.25	91.95	96.56
Sharma et al. (2017) [11]	F: 3,750 NF: 3,750	TQWT, entropy, LS-SVM	10-fold	95	-	-
Gupta et al. (2017) [12]	F: 3,750 NF: 3,750	FAWT, entropy, Kruskal-Wallis test, LS-SVM	10-fold	94.41	93.25	95.57
Bhattacharyya et al. (2017) [13]	F: 50 NF: 50	TQWT, entropy, LS-SVM	10-fold	84.67	83.86	85.46
Sriraam et al. (2017) [15]	F: 3,750 NF: 3,750	Statistical, frequency-based, entropy, FD, Wilcoxon test, SVM	10-fold	92.15	94.56	89.74
Arunkumar et al. (2017) [16]	F: 50 NF: 50	Entropies, non-nested generalized exemplars	10-fold	98	100	96
Bhattacharyya et al. (2018) [14]	F: 50 NF: 50	EWT, RPS, CTM, LS-SVM	10-fold	90	88	92
Present study	F: 3,750 NF: 3,750	Bispectrum, DFA, entropies, FD, Hjorth parameters, Hurst exponent Kolmogorov complexity, LLE, LZC, LS-SVM (Total of 23 features used)	10-fold	87.93	89.97	85.89

6. Future Development

In future development, the CAD system will be combined with deep learning techniques. Deep learning is a sophisticated machine learning method, inspired by the neural network structure in the human brain. It is an established discipline that is employed in diverse research fields including speech recognition [58], object recognition [59], structural damage detection [60], and for diagnosis using physiological signals [61, 62, 63, 64, 65] and medical images [66]. It is noted that deep learning eliminates the need for feature extraction, selection, and classification. The model can self-learn via the training of the data. Therefore, deep learning techniques can be explored to improve the design of CAD systems, and to accurately localize the epileptogenic area of the brain using EEG signals. Additionally, application of a web-based implementation can be integrated with the proposed deep learning CAD system. With a web-based implementation, clinicians can analyze the EEG signals via cloud storage, and diagnoses made would be sent back to the local server almost instantaneously.

Moreover, as part of the future work, the authors propose to incorporate both MRI images and EEG signals to identify the epileptogenic area of the brain. Providing two sources (image and signal) will ensure a more accurate localization of the epileptogenic zone. The concept of combining two or more different inputs together for analysis is termed radiomics. It is the extraction of a large feature set to gather further information for diagnosis of specific health conditions [67]. Consequently, the authors plan to implement the CAD system with radiomics methods, whereby different quantitative features are extracted from medical images to identify the epileptogenic zone [67, 68].

7. Conclusion

This study contrasts the performance of *nine* nonlinear features in differentiating two types of EEG signals. It can be seen that these nonlinear features can detect minute changes in the EEG signals of two (NF and F) classes. The developed CAD model has the potential to be deployed in clinical settings, to aid in offering an objective second opinion for detection of NF versus F EEG signals. Also, unique nonlinear plots have been proposed to discriminate the two classes visually.

8. References

[1] R. S. Fisher, W. v. E. Boas, W. Blume, C. Elger, P. Genton, P. Lee and J. J. Engel, "Epileptic seizures and epilepsy: definitions proposed by the international league against epilepsy (ILAE) and the international bureau for epilepsy (IBE)," *Epilepsia,* vol. 46, no. 4, pp. 470-472, 2005.

[2] World Health Organization, "World Health Organization," 08 02 2018. [Online]. Available: http://www.who.int/news-room/fact-sheets/detail/epilepsy. [Accessed 12 07 2018].

[3] S. Pati and A. V. Alexopoulos, "Pharmacoresistant epilepsy: from pathogenesis to current and emerging therapies," *Cleveland Clinic Journal of Medicine,* vol. 77, no. 7, pp. 457-467, 2010.

[4] H. L. Weiner and J. I. Sirven, "Epilepsy Foundation," 25 August 2013. [Online]. Available: https://www.epilepsy.com/learn/treating-seizures-and-epilepsy/surgery/types-surgeries. [Accessed 23 July 2018].

[5] R. G. Andrzejak, K. Schindler and C. Rummel, "Nonrandomness, nonlinear dependence and nonstationarity of electroencephalographic recordings from epilepsy patients," *Physical Review E,* vol. 86, p. 046206, 2012.

[6] R. Sharma, R. B. Pachori and U. R. Acharya, "Application of entropy measures on intrinsic mode functions for the automated identification of focal electroencephalogram signals," *Entropy,* vol. 17, pp. 669-691, 2015.

[7] R. Sharma, R. B. Pachori and U. R. Acharya, "An integrated index for the identification of focal electroencephalogram signals using discrete wavelet transform and entropy measures," *Entropy,* vol. 17, pp. 5218-5240, 2015.

[8] M. Sharma, A. Dhere, R. B. Pachori and U. R. Acharya, "An automatic detection of focal EEG signals using new class of time-frequency localized orthogonal wavelet filter banks," *Knowledge-Based Systems,* vol. 118, pp. 217-227, 2017.

[9] S. Deivasigamani, C. Senthilpari and H. Y. Wong, "Classification of focal and nonfocal EEG signals using ANFIS classifier for epilepsy detection," *International Journal of Imaging Systems and Technology,* vol. 26, no. 4, pp. 277-283, 2016.

[10] A. B. Das and M. I. H. Bhuiyan, "Discrimination and classification of focal and non-focal EEG signals using entropy-based features in the EMD-DWT domain," *Biomedical Signal Processing and Control,* vol. 29, pp. 11-21, 2016.

[11] R. Sharma, M. Kumar, R. B. Pachori and U. R. Acharya, "Decision support system for focal EEG signals using tunable-Q wavelet transform," *Journal of Computational Science,* vol. 20, pp. 52-60, 2017.

[12] V. Gupta, T. Priya, A. K. Yadav, R. B. Pachori and U. R. Acharya, "Automated detection of focal EEG signals using features extracted from flexible analytic wavelet transform," *Pattern Recognition Letters,* vol. 94, pp. 180-188, 2017.

[13] A. Bhattacharyya, R. B. Pachori and U. R. Acharya, "Tunable-Q wavelet transform based multivariate sub-band fuzzy entropy with application to focal EEG signal analysis," *Entropy,* vol. 19, no. 3, p. 99, 2017.

[14] A. Bhattacharyya, M. Sharma, R. B. Pachori, P. Sircar and U. R. Acharya, "A novel approach for automated detection of focal EEG signals using empirical wavelet transform," *Neural Computing and Applications,* vol. 29, no. 8, pp. 47-57, 2018.

[15] N. Sriraam and S. Raghu, "Classification of focal and non focal epileptic seizures using multi-features and SVM classifier," *Journal of Medical Systems,* vol. 41, p. 160 (14 pages), 2017.

[16] N. Arunkumar, K. Ramkumar, V. Venkatraman, E. Abdulhay, S. L. Fernandes, S. Kadry and S. Segal, "Classification of focal and non focal EEG using entropies," *Pattern Recognition Letters ,* vol. 94, pp. 112-117, 2017.

[17] R. J. Hyndman and G. Athanasopoulos, "8.1 Stationarity and differencing," in *Forecasting: Principles and practices*, Melbourne, Australia, OTexts, 2013.

[18] U. R. Acharya, S. V. Sree, G. Swapna, R. J. Martis and J. S. Suri, "Automated EEG analysis of epilepsy: A review," *Knowledge-Based Systems,* vol. 45, pp. 147-165, 2013.

[19] C. K. Peng, S. V. Buldyrev, S. Havlin, M. Simons, H. E. Stanley and A. L. Goldberger, "Mosaic organization of DNA nucleotides," *Physical Review E,* vol. 49, no. 2, pp. 1685-1689, 1994.

[20] U. R. Acharya, H. Fujita, V. K. Sudarshan, S. Bhat and J. E. W. Koh, "Application of entropies for automated diagnosis of epilepsy using EEG signals: A review," *Knowledge-Based Systems,* vol. 88, pp. 85-96, 2015.

[21] S. D. Wu, C. W. Wu, K. Y. Lee and S. G. Lin, "Modified multiscale entropy for short-term time series analysis," *Physica A,* vol. 392, pp. 5865-5873, 2013.

[22] J. S. Richman and J. R. Moorman, "Physiological time-series analysis using approximate entropy and sample entropy," *American Journal of Physiological - Heart and Circulatory Physiology,* vol. 278, no. 6, pp. 2039-2049, 2000.

[23] S. M. Pincus, "Approximate entropy as a measure of system complexity," *Proceedings of the National Academy of Sciences of the United States of America,* vol. 88, pp. 2297-2301, 1991.

[24] B. Kosko, "Fuzzy entropy and conditioning," *Information Sciences,* vol. 40, no. 2, pp. 165-174, 1986.

[25] A. N. Kolmogorov, "New metric invariant of transitive dynamical systems and endomorphisms of Lebesgue spaces," *Doklady of Russian Academy of Sciences,* vol. 119, pp. 861-864, 1958.

[26] A. Renyi, “On measures of entropy and information,” in *Fourth Berkeley Symposium*, 1961.

[27] C. E. Shannon, “A mathematical theory of communication,” *The Bell System Technical Journal,* vol. 27, no. 3, pp. 379-423, 1948.

[28] C. L. Nikias and J. M. Mendel, “Higher-order spectra analysis,” *IEEE Signal Processing Magazine,* vol. 10, no. 3, pp. 10-37, 1993.

[29] C. Tsallis, “Possible generalization of Boltzmann-Gibbs statistics,” *Journal of Statistical Physics,* vol. 52, no. 1-2, pp. 479-487, 1988.

[30] O. A. Rosso, S. Blanco, J. Yordanova, V. Kolev, A. Figliola, M. Schurmann and E. Basar, “Wavelet entropy:a new tool for analysis of short duration brain electrical signals,” *Journal of Neuroscience Methods,* vol. 105, pp. 65-75, 2001.

[31] C. Bandt and B. Pompe, “Permutation entropy: a natural complexity measure for time series,” *Physical Review Letters,* vol. 88, no. 17, p. 174102, 2002.

[32] B. B. Mandelbrot, Geometry of nature, San Francisco: Freeman, 1983.

[33] B. Hjorth and A. B. Elema-Schonander, “EEG analysis based on time domain properties,” *Electroencephalography and Clinical Neurophysiology,* vol. 29, pp. 306-310, 1970.

[34] H. E. Hurst, “Methods of using long-term storage in reservoirs,” *Proceedings of the Institution of Civil Engineers,* vol. 5, no. 5, pp. 519-543, 1956.

[35] A. Kolmogorov, “On tables of random numbers,” *Theoretical Computer Science,* vol. 207, no. 2, pp. 387-395, 1998.

[36] M. Rosenstein, J. J. Colins and C. J. Luca, “A practical method for calculating largest Lyapunov exponents from small data sets,” *Physica D,* vol. 65, pp. 117-134, 1993.

[37] J. Ziv and A. Lempel, “A universal algorithm for sequential data compression,” *IEEE Transactions on Information Theory,* vol. 23, pp. 337-343, 1977.

[38] J. P. Zbilut and C. L. J. Webber, “Embeddings and delays as derived from quantification of recurrence plots,” *Physics Letters A,* vol. 171, no. 3-4, pp. 199-203, 1992.

[39] J. P. Eckmann, S. O. Kamphorst and D. Ruelle, “Recurrence plots of dynamical systems,” *Europhysics Letters,* vol. 4, no. 9, p. 973, 1987.

[40] N. Marwan, “A historical review of recurrence plots,” *The European Physical Journal Special Topics,* vol. 164, no. 1, pp. 3-12, 2008.

[41] N. Marwan, M. C. Romano, M. Thiel and J. Kurths, “Recurrence plots for the analysis of complex systems,” *Physics Reports,* vol. 438, no. 5-6, pp. 237-329, 2007.

[42] Student, “The probable error of a mean,” *Biometrika,* vol. 6, no. 1, pp. 1-25, 1908.

[43] S. Theodoridis and K. Koutroumbas, “Feature selection,” in *Pattern recognition 2nd edition*, San Diego, CA, USA, Academic Press, 2003, pp. 163-205.

[44] T. Kailath, “The divergence and Bhattacharyya distance measures in signal selection,” *IEEE Transactions of Communication Technology,* vol. 15, pp. 52-60, 1967.

[45] D. R. Derryberry, S. B. Schou and W. J. Conover, “Teaching rank-based tests by emphasizing structural similarities to corresponding parametric tests,” *Journal of Statistics Education,* vol. 18, pp. 1-19, 2010.

[46] W. H. Kruskal and W. A. Wallis, “Use of ranks in one-criterion variance analysis,” *Journal of the American Statistical Association,* vol. 47, no. 260, pp. 583-621, 1952.

[47] J. A. K. Suykens and J. Vandewalle, “Least squares support vector machine classifiers,” *Neural Processing Letters,* vol. 9, no. 3, pp. 293-300, 1999.

[48] J. S. R. Jang, “ANFIS: adaptive-network-based fuzzy inference system,” *IEEE Transactions on Systems, Man, and Cybernetics,* vol. 23, no. 3, pp. 665-685, 1993.

[49] T. M. Cover and P. E. Hart, “Nearest neighbor pattern classification,” *IEEE Transactions of Information Theory,* vol. 13, no. 1, pp. 21-27, 1967.

[50] B. Martin, “Instance-based learning: nearest neighbor with generalization,” Department of Computer Science, University of Waikato, Hamilton, New Zealand, 1995.

[51] N. E. Huang, Z. Shen, S. R. Long, M. C. Wu, H. H. Shih, Q. Zheng, N. C. Yen, C. C. Tung and H. H. Liu, “The empirical mode decomposition and the Hilbert spectrum for nonlinear and non-stationary time series analysis,” *Proceedings of the Royal Society,* vol. 454, pp. 903-995, 1998.

[52] S. Mallat, “A theory for multi-resolution signal decomposition: the wavelet representation,” *IEEE Transactions on Pattern Analysis and Machine Intelligence,* vol. 11, no. 7, pp. 674-693, 1989.

[53] N. Kingsbury, “The dual-tree complex wavelet transform: a new technique for shift invariance and directional filters,” in *Proceedings of the 8th IEEE Digital Signal Processing Workshop*, Utah, 1998.

[54] M. Vetterli and C. Herley, “Wavelets and filter banks: theory and design,” *IEEE Transactions on Signal Processing,* vol. 40, no. 9, pp. 2207-2232, 1992.

[55] I. W. Selesnick, “Wavelet transform with tunable Q-factor,” *IEEE Transactions on Signal Processing,* vol. 59, no. 8, pp. 3560-3575, 2011.

[56] I. Bayram, “An analytic wavelet transform with a flexible time-frequency covering,” *IEEE Transactions on Signal Processing,* vol. 61, no. 5, pp. 1131-1142, 2013.

[57] J. Gilles, “Empirical wavelet transform,” *IEEE Transactions on Signal Processing,* vol. 61, no. 16, pp. 3999-4010, 2013.

[58] A. Graves, A. Mohamed and G. E. Hinton, “Speech recognition with deep recurrent neural networks,” in *IEEE International Conference on Acoustics, Speech and Signal Processing*, Vancouver, BC, Canada, 2013.

[59] A. Krizhevsky, I. Sutskever and G. E. Hinton, “ImageNet classification with deep convolutional neural networks,” in *Proceedings of the 25th International Conference on Neural Information Processing Systems*, Lake Tahoe, Nevada, 2012.

[60] Y. Z. Lin, Z. H. Nie and H. W. Ma, “Structural damage detection with automatic feature-extraction through deep learning,” *Computer-Aided Civil and Infrastructure Engineering,* vol. 32, no. 12, pp. 1025-1046, 2017.

[61] U. R. Acharya, S. L. Oh, Y. Hagiwara, J. H. Tan, H. Adeli and D. P. Subha, “Automated EEG-based screening of depression using deep convolutional neural network,” *Computer Methods and Programs in Biomedicine,* vol. 161, pp. 103-113, 2018.

[62] U. R. Acharya, S. L. Oh, Y. Hagiwara, J. H. Tan and H. Adeli, “Deep convolutional neural network for the automated detection and diagnosis of seizure using EEG signals,” *Computers in Biology and Medicine,* vol. https://doi.org/10.1016/j.compbiomed.2017.09.017, 2017.

[63] U. R. Acharya, H. Fujita, S. L. Oh, Y. Hagiwara, J. H. Tan and M. Adam, “Automated detection of arrhythmias using different intervals of tachycardia ECG segments with convolutional neural network,” *Information sciences,* vol. 405, pp. 81-90, 2017.

[64] U. R. Acharya, S. L. Oh, Y. Hagiwara, J. H. Tan, M. Adam, A. Gertych and R. S. Tan, “A deep convolutional neural network model to classify heartbeats,” *Computers in biology and medicine,* vol. 89, pp. 389-396, 2017.

[65] U. R. Acharya, H. Fujita, S. L. Oh, Y. Hagiwara, J. H. Tan and M. Adam, “Application of deep convolutional neural network for automated detection of myocardial infarction using ECG signals,” *Information Sciences,* vol. 415, pp. 190-198, 2017.

[66] J. H. Tan, S. V. Bhandary, S. Sivaprasad, Y. Hagiwara, A. Bagchi, U. Raghavendra, A. K. Rao, B. Raju, N. S. Shetty, A. Gertych, K. C. Chua and U. R. Acharya, “Age-related Macular Degeneration detection using deep convolutional neural network,” *Future Generation Computer Systems,* vol. 87, pp. 127-135, 2018.

[67] P. Lambin, E. Rios-Velazquez, R. Leijenaar, S. Carvalho, R. G. v. Stiphout, P. Granton, C. M. Zegers, R. Gillies, R. Boellard, A. Dekker and H. J. Aerts, “Radiomics: extracting more information from medical images using advanced feature analysis,” *European Journal of Cancer,* vol. 48, no. 4, pp. 441-446, 2012.

[68] U. R. Acharya, Y. Hagiwara, V. K. Sudarshan, W. Y. Chan and K. H. Ng, “Towards precision medicine: from quantitative imaging to radiomics,” *Journal of Zhejiang University, Science B,* vol. 19, no. 1, pp. 6-24, 2018.